FINAL TECHNICAL REPORT

Department of Energy, Office of **High Energy Physics**
Grant #: **DE-SC0015500**

eSHIVA in IOTA:
Experiment on Stochasticity in High Intensity Variable Accelerators

PI: Prof. *Swapan Chattopadhyay*
co-PI: Prof. *Béla Erdélyi*
Department of Physics
Northern Illinois University
DeKalb, IL 60115
Phone: (815) 753- ????
Fax (815) 753-8565;
E-mail: ?

DUNS #: 0017455120000
Northern Illinois University
DeKalb, IL 60115

Grant period: **05/01/2016 – 03/30/2019**

Submission date: **September 13, 2019**

Task I : Integrable Discretization of Integrable Hamiltonian Systems

1. EXECUTIVE SUMMARY

Nonlinear integrable optics, the basis of IOTA, is a very special form of Hamiltonian system, called completely integrable. The consequences are many, most importantly the absence of fixed points that are in one-to-one correspondence with (overlapping) resonances. This, in turn, does not limit the dynamic aperture and allows large amplitude dependent tune shifts without adverse effects. In fact, it helps significantly in alleviating issues with collective instabilities.

We developed and tested different numerical methods to give a more complete picture of the dynamics of integrable and near-integrable nonlinear Hamiltonian systems consisting of motion of charged particles in electromagnetic fields. Comparison of the results allowed us to discern real phenomena from numerical artifacts and come up with conclusions that will facilitate pushing the intensity frontier in beam dynamics even further for the benefit of the accelerator community as a whole and society as the consequence of the science and technological advancements it will make possible.

We concluded that, while novel structure preserving integrators would be ideal, symplectic methods under mild restrictions offer adequate invariant preservation. We especially highlighted the very good performance of the Stormer-Verlet method at low accuracy and a modified Lobatto method at high accuracy for the Integrable Optics Test Accelerator (IOTA). However, we showed that symplectic integrators are limited by numerically induced resonances, which make interpretation of some simulation results challenging. These limitations and workarounds have been addressed.

2. ACCOMPLISHEMENTS

While it is straightforward to understand the dynamics of integrable systems in theory, numerical solutions needed for modeling and simulations are not immediate descendants of these theories. The issue is—well known in the mathematical field of numerical geometric integration—that most off-the-shelf numerical integrators do not preserve important properties of the continuous-time system, including integrability. In the beam physics and accelerator science community it is highly appreciated that the Hamiltonian property is essential to be preserved in long-term simulations; hence the widespread application of symplectic integrators and symplectification methods. Not known are integrators that preserve integrability.

One specific aim of this project was to understand the effect of application of non-symplectic and symplectic integrators to integrable systems. The second specific aim was to develop new methods that explicitly preserve integrability. This is a cutting edge topic in the applied mathematics community too. For example, according to the definition of integrable discretization, only very recently it was discovered that a 25-year-old integrator has remarkable integrability-preservation properties when applied to cubic Hamiltonians in the plane.

A first study of polynomial integrable Hamiltonian systems showed that non-symplectic methods are not competitive; even if some of them are accurate enough point-wise, secular drifts in Hamiltonian and invariant are routinely observed. Moreover, Kahan's method, for which we had high hopes, failed to behave symplectically for complicated enough Hamiltonian systems. These results are summarized in Table 1. That's why, we dropped further studies of non-symplectic and Kahan's method.

Table 1. Results for testing a polynomial integrable Hamiltonian system integration, where 100 seconds of time flow is run with an error bound of 5×10^{-6}.

Method	h	Hamiltonian error	Invariant error	Time
symplectic Euler	0.01605055	5×10^{-6}	4.70523×10^{-7}	0.628
Stormer-Verlet	0.0698802	5×10^{-6}	4.69503×10^{-7}	1.204
Implicit Midpoint	0.0247594	5×10^{-6}	4.70749×10^{-7}	2.04
RK2	0.307825	5×10^{-6}	1.57272×10^{-7}	0.372
RK3	0.671024	5×10^{-6}	3.08871×10^{-8}	0.40
Lobatto 2	0.307825	5×10^{-6}	1.57272×10^{-7}	0.344
Lobatto 3	0.671024	5×10^{-6}	3.08871×10^{-8}	0.336
Kahan method	0.0108558	5×10^{-6}	4.02039×10^{-6}	0.544

Turning our attention to the IOTA Hamiltonian, and concentrating only on symplectic integrators, we observed that efficiency depends on the sought accuracy. We obtained that at low to medium accuracies Stormer-Verlet is optimal, while as the accuracy tends towards machine precision Lobatto of relatively high orders become increasingly optimal. These results at low, medium, and high accuracy, respectively, are shown in Tables 2-4.

Table 2. Comparison of symplectic methods for IOTA at low accuracy.

Method	h	Hamiltonian error	Invariant error	Time
sympletic Euler	0.132168	0.000459462	0.0010	1.592
Stormer-Verlet	0.530168	0.000606631	0.0010	0.916
Implicit Midpoint	0.533055	0.00099999	0.000957827	9.372
RK2	0.896155	0.000538253	0.0010	37.78
RK3	1.6439	0.000523777	0.000998863	58.984
Lobatto 2	0.896155	0.000538253	0.0010	10.936
Lobatto 3	1.6439	0.000523777	0.000998863	13.488
LT splitting	0.0222919	0.00076075	0.0010	46.156

Table 3. Comparison of symplectic methods for IOTA at medium accuracy.

Method	h	Hamiltonian error	Invariant error	Time
sympletic Euler	0.000029669	2.29911×10^{-11}	4.99976×10^{-11}	537.44
Stormer-Verlet	0.000318416	4.87156×10^{-11}	4.32441×10^{-11}	147.8
Implicit midpoint	0.000113953	4.99981×10^{-11}	4.44692×10^{-11}	4146.3
RK2	0.0202143	4.99995×10^{-11}	4.15239×10^{-11}	146.664
RK3	0.138829	4.49783×10^{-11}	4.99994×10^{-11}	68.296
Lobatto 2	0.0202143	4.99994×10^{-11}	4.15237×10^{-11}	40.656
Lobatto 3	0.138829	4.49784×10^{-11}	4.99993×10^{-11}	12.86

Table 4. Comparison of symplectic methods for IOTA at high accuracy.

Method	h	Hamiltonian error	Invariant error	Time
Lobatto 2	0.000891667	6.38378×10^{-16}	9.71445×10^{-16}	818.596
Lobatto 3	0.0174	3.05311×10^{-16}	5.27356×10^{-16}	117.264
Lobatto 4	0.06	3.46945×10^{-16}	2.22045×10^{-16}	82.584
Lobatto 5	0.154	3.19189×10^{-16}	2.498×10^{-16}	45.012

While symplectic methods did not show secular drifts over long tracking time, they had their own problems; the most significant being destruction of integrability. In other words, when even the best symplectic integrator of any order and any reasonable time step is applied to IOTA, for some initial conditions, called resonant, the invariant error becomes much larger than for its surrounding initial conditions. This sensitivity to initial conditions resembles resonant and chaotic motion in non-integrable systems, but they are not real. That is, the methods do not introduce non-physical behavior, and hence could be mistaken for realistic effects that limit the dynamic aperture, for example, or other phenomena seen in accelerators based on non-integrable Hamiltonians. The following couple of figures give an overview of this situation. See Figures 1 and 2.

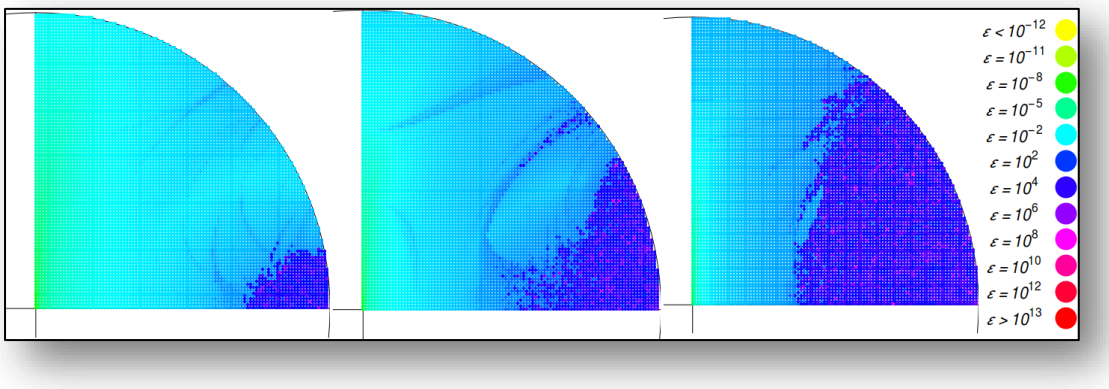

Figure 1. Numerical artifacts in symplectic integration with large time steps: artificial resonances obtained from sampling with the Stormer-Verlet method with step sizes 0.6 and 1, and 1.5.

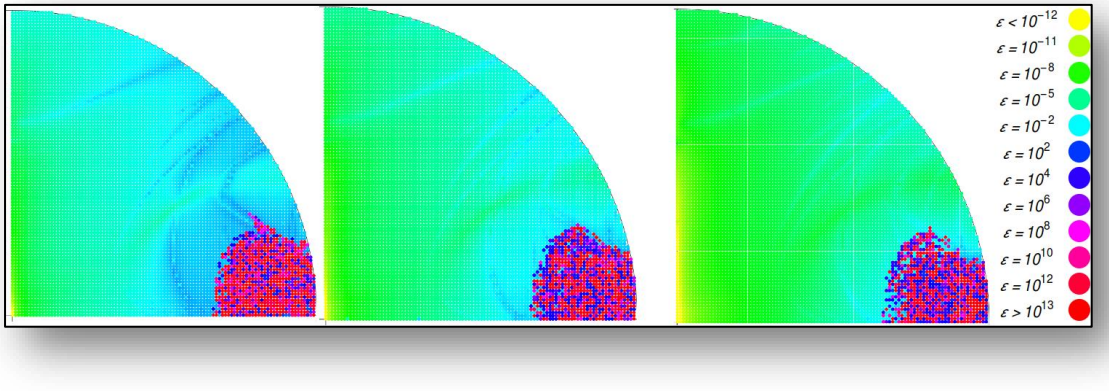

Figure 2. Same as Fig. 1, but sampling with the Lobatto 3, 4 and 5 methods, respectively, from left to right, each with step size 1.

The conclusion is that a reasonably high order Lobatto with various time steps gives the best way to interpret correctly the simulation results of IOTA or other integrable Hamiltonian-based accelerator systems.

The results on applying this insight to normal form analysis of IOTA gave mixed results. While the numerical methods themselves were carefully chosen and understood, as described in earlier paragraphs, the normal form method itself turned out to converge slowly. We traced back this behavior to the slow multipole expansion convergence of the nonlinear magnet's field. See Figure 3. As a consequence, we were able to study the nonlinear dynamics in about 70-80% of the physical aperture of IOTA. While this is interesting in itself, unfortunately it leaves out the most nonlinear and hence most intricate region of phase space. For example, at order 14, at magnetic field error level of ~1% we obtained Figure 3.

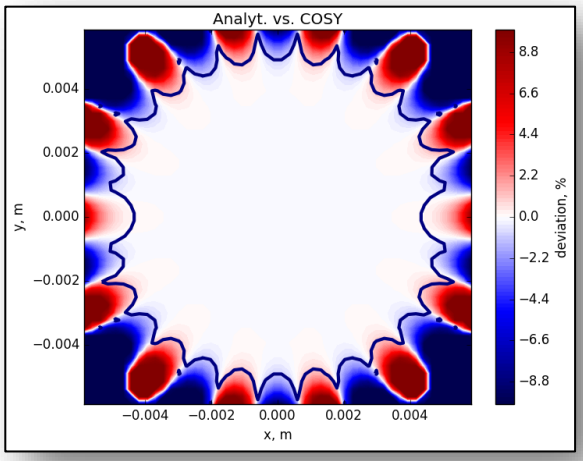

Figure 3. 1% error contour of the magnitude of the magnetic field in the nonlinear magnet obtained from a multipole expansion of order 14.

The usual normal form outcomes of amplitude-dependent tune shifts and resonance strengths are shown in Figures 4 and 5. These results show that the large tune footprints necessary for beneficial operation of IOTA can be attained, but the full aperture needs to be filled with beam to reach the most nonlinear regions of phase space. The resonance strength study is inconclusive due to its slow convergence. While convergence is guaranteed by theory, the slow convergence of the field expansion has most of its effect on the slow convergence of the normalized resonance driving terms. These resonances show the resilience or sensitivity of integrable systems to perturbations, and thus it is of utmost importance to understand them in order to ensure the large dynamic apertures needed for stable operation.

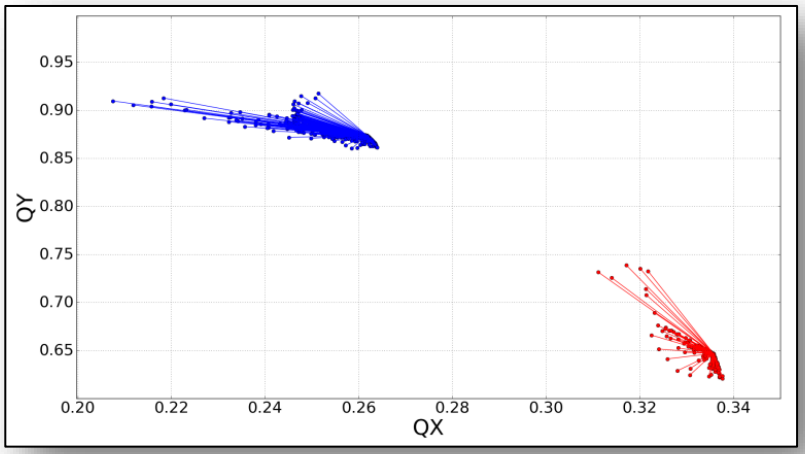

Figure 4. Horizontal and vertical tune footprints obtained by normal form corresponding to ~80% of the physical aperture.

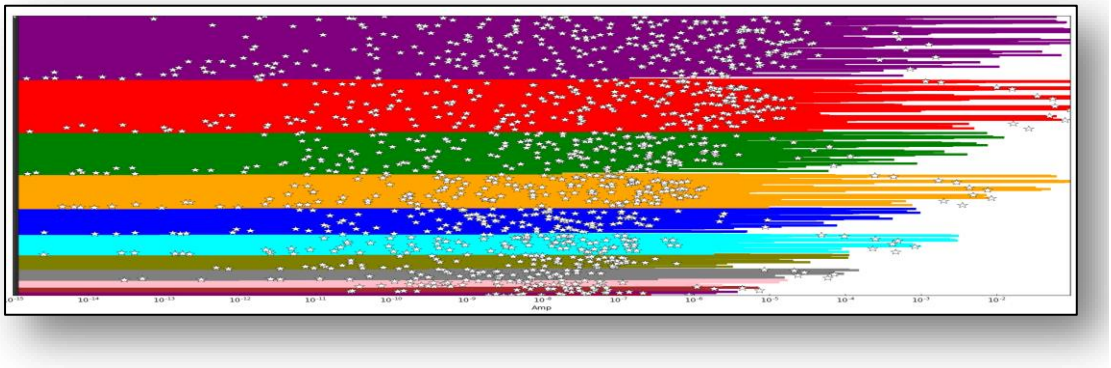

Figure 5. Resonance driving terms of all orders up to 14 (colored bars) and their normalization to 80% amplitude (dots) shows that convergence has not been achieved yet at this order and amplitude.

As a synergistic research project, we explored the alternative theory of giving up on integrability and just taking any existing system and devising methods of increasing their dynamic aperture. This also turned out to be a most difficult problem, leading us to applications of a state-of-the-art branch of mathematics named stable polynomials. We summarized the current state of DA enlargement in an arXiv report.

To summarize, motivated by novel accelerators characterized by some magnetic fields never used before in practice, which make the appropriate mathematical models consisting of nonlinear completely integrable Hamiltonian systems, we undertook a systematic search for the best numerical discretization of the corresponding differential equations by a variety of numerical integration methods. The prime example of such systems is the Integrable Optics Test Accelerator (IOTA) at Fermilab, but the integrators have been tested on simpler, homogeneous polynomial integrable Hamiltonians in 4D too. The categories of numerical methods tested comprised non-symplectic (including adaptive realizations of various orders and number of steps) and symplectic (various orders, including splitting and composition) methods. We also tested a non-conventional method of Kahan, a conjugate symplectic method that produces provably integrable discretizations of cubic Hamiltonians of the plane. The performance of the integrators was judged based on two main criteria: correct qualitative behavior of the invariants in step one, and runtime for given a priori error bounds on the invariants in step two.

As expected, non-symplectic methods were disappointing. The invariants had secular drifts irrespective of the integrator used. Although high orders, small time steps, and adaptivity can alleviate some of the problems, it is only a matter of time before the secular, non-physical changes spoil the important properties of integrable Hamiltonian systems. Moreover, arbitrary small time steps lead to numerical instabilities or underflow. Also, Kahan's method, unfortunately, behaves effectively in a non-symplectic manner for the Hamiltonians of interest to us.

Symplectic methods give much better results in general. For sufficiently small time steps the invariants do not drift. Oscillations are observed, with amplitudes inversely proportional to the order and directly proportional to the time step size. The time steps needed to maintain an upper bound on invariant errors depend on the details of the systems, and the specific initial conditions. For IOTA, there is a region near the poles that is most sensitive to the details of the integrator, while near the origin the dynamics is tamer, as expected from the modest magnitude of the field nonlinearities there. The most efficient symplectic integrator is different as a function of the required accuracies. For low to medium accuracy we recommend the Stormer-Verlet method, while for high accuracy, up to machine precision, we recommend a reasonably high order (around 4-5) Lobatto method.

It is important to note that symplectic integrators are not a panacea. They introduce numerical artifacts to integrable systems that look physical. Most important are the numerical resonances generated by the perturbation of the original systems by the symplectic discretization. The artifacts depend on the method employed, their order, and the time step size. Once the type of the method is selected, it is indicated that a reasonably high order is used with a sufficiently small step size (but not too small). We observed convergence of the artifacts with order at fixed time step. We also observed the theoretically expected results that as the time step goes to zero, the measure of non-resonant time steps tends to one. Another practically useful recommendation is to run simulations with at least two different time steps; the ensuing qualitative resonance web differences are likely due to numerical artifacts.

Finally, under these recommendations, are symplectic integrators good enough to draw reliable conclusions from simulations? We trust the answer is yes. In any case, it is likely it is the best we can do, since complete integrability is very fragile, and even the best integrator—symplectic or not—introduces perturbations through the discretization that spoils the integrability, because even very close, nearby Hamiltonians cease to be integrable. We are able to simulate with confidence systems that are robust under arbitrarily small perturbations, and these systems are the ones relevant in practice, since small errors are unavoidable in building these systems.

3. PRODUCTS

Refereed publications supported by the grant:

1. S. Rexford and B. Erdelyi, *Numerical discretization of completely integrable nonlinear Hamiltonian systems*, Phys. Rev. Accel. Beams **21(11)**, 114601 (20 pp.) – Published 14 November 2018

Conference papers, reports and presentations:

1. H. D. Schaumburg and B. Erdelyi, *A Study on a New Method of Dynamic Aperture Enlargement*, arXiv: 1809.03418, pp. 68 (2018)

2. A. Patapenka, B. Erdelyi, *Single particle beam dynamics studies for the IOTA ring with COSY Infinity*, Fermilab Workshop on Megawatt Rings & IOTA/FAST Collaboration Meeting, Fermilab, Batavia, IL, May 7-10, 2018.
3. B. Erdelyi, *Normal form approach to and nonlinear optics analysis of the IOTA ring*, 13th International Computational Accelerator Physics Conference, Key West, FL, October 20-24, 2018.

4. PARTICIPANTS

1. **Name:** Bela Erdelyi
2. **Project Role:** Principal Investigator
3. **Nearest person months worked:** 3
4. **Contribution to Project:** technical leadership of the task on integrable discretization

1. **Name:** Scott Rexford
2. **Project Role:** Graduate Research Assistant
3. **Nearest person months worked:** 6
4. **Contribution to Project:** developed numerical methods to test their integrable discretization performance

1. **Name:** Herman Schaumburg
2. **Project Role:** None (NIU postdoc)
3. **Nearest person month worked:** 0
4. **Contribution to Project:** synergistic research efforts on increasing dynamic aperture for accelerators such as IOTA, i.e. (near-)integrable

1. **Name:** Andrei Patapenka
2. **Project Role:** None (NIU postdoc)
3. **Nearest person month worked:** 0
4. **Contribution to Project:** synergistic research efforts on normal form analysis of accelerators such as IOTA, i.e. (near-)integrable

Task II: Nonlinear tune-shift measurements in IOTA and simulation, design and fabrication of Gas Jet Monitoring system to measure beam profile and diffusive halo in IOTA

1. EXECUTIVE SUMMARY

The nonlinear integrable optics test accelerator IOTA at Fermilab -- a very special experimental accelerator designed to investigate nonlinear optics under severe space-charge conditions – has recently completed its construction and initial commissioning of the ring has begun. We report first, under 2 (a) below: the progress on the nonlinear tune-shift measurements for various values of the nonlinear strength potential and their comparison with theoretical expectations, thus benchmarking the nonlinear characteristics of the ring; then, under 2 (b) below: the progress on simulation and design of a gas-jet monitor to measure beam profile and in particular its diffusive halo, expected to develop during stochastic diffusion of large amplitude particles under nonlinear forces of the magnetic lattice and Coulomb space-charge.

Since the development of a proton beam source in IOTA is delayed and to be completed only in the future pending financial support, the gas-jet monitor is planned for testing with real proton beams elsewhere at Fermilab (e.g. in the Main Injector or PIP-II source possibly). Once proton beams are available in IOTA, the understanding of the nonlinear properties of IOTA combined with the developed gas-jet monitor, will enable a thorough experimental analysis of nonlinear stochastic diffusion in IOTA nonlinear ring, and boosted by proper theoretical understanding of the same.

2. ACCOMPLISHEMENTS

(a) Nonlinear Tune-shift Merasurements in the Integrable Optics Test Accelerator:

The first experimental run of Fermilab's Integrable Optics Test Accelerator (IOTA) ring (shown below) was aimed at testing the concept of nonlinear integrable beam optics. In this report we present the preliminary results of the studies of a nonlinear focusing system with two invariants of motion realized with the special elliptic-potential magnet. The key measurement of this experiment was the horizontal and vertical betatron tune shift as a function of transverse amplitude. A vertical kicker strength was varied to change the betatron amplitude for several values of the nonlinear magnet strength. The turn-by-turn positions of the 100 MeV electron beam at twenty-one beam position monitors around the ring were captured and used for the analysis of phase-space trajectories.

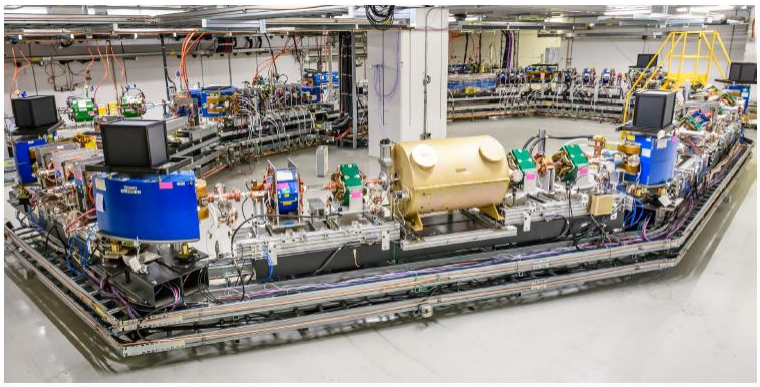

IOTA (Integrable Optics Test Accelerator) ring at Fermilab

The tune diagram in vertical and horizontal planes was explored by varying the strength 't' of the specially fabricated nonlinear magnet mentioned above.

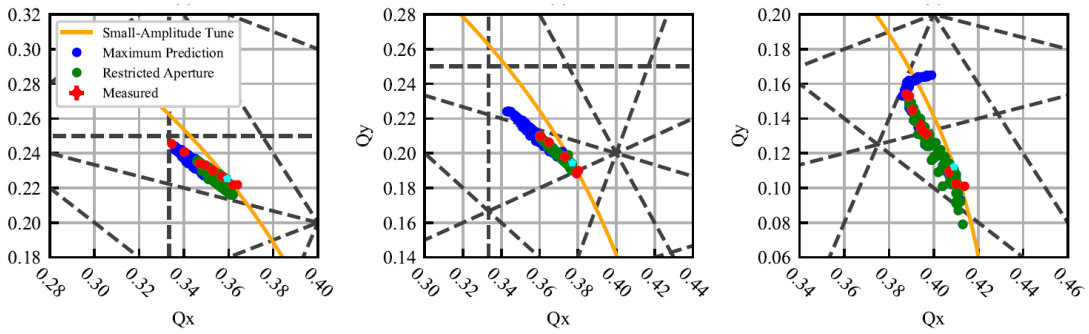

The 'Tune'- diagram at various t-strength values with model tunes and its mechanical restrictions at various nonlinear potential strengths, characterized by a scaled parameter 't'. (a) t=0.2179, (b) t=0.2903 and (c) t=0.4324 are shown above.

The small-amplitude tunes for various strengths of the nonlinear potential were also measured. Small-amplitude tune diagram of measured and theoretical tunes at various values of the nonlinear potential strength parameter 't' are shown below.

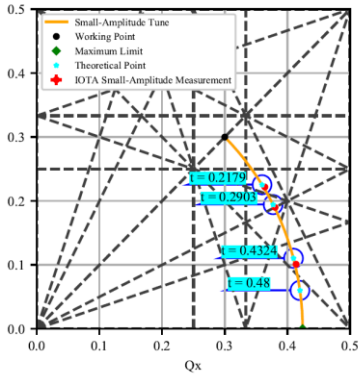

Amplitude-dependent nonlinear tune-shift for: (a) Vertical tune and (b) horizontal tune versus vertical kick at a certain 'scaled' nonlinear potential strength parameter t=0.4324 are shown below.

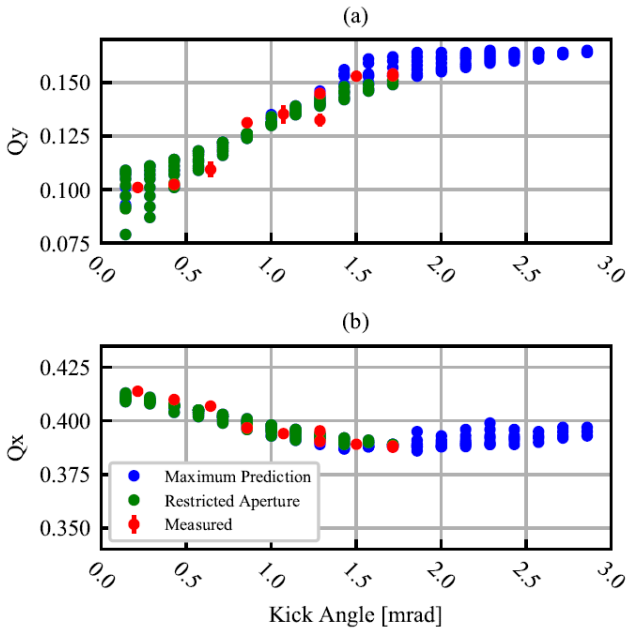

The above database of complete nonlinear characteristics of the bare nonlinear IOTA ring without any space-charge-dominated beam in it will be used to facilitate studies of nonlinear diffusion in presence of a high intensity low-energy proton beam in IOTA, with the aid of a Gas Jet Beam Profile monitor described and reported below under 2(b).

(b) Development of a gas sheet beam profile monitor for IOTA:

A nitrogen gas sheet will be used to measure the two-dimensional transverse profile of the 2.5 MeV proton beam in IOTA. The beam lifetime is limited by the interaction with the gas, thus a minimally invasive instrument is required. To produce a gas sheet with the desired density and thickness, various nozzle types are being investigated, including rectangular capillary tubes for gas injection and skimmers for final shaping of the gas. It is essential to meet vacuum requirements in the interaction chamber while maintaining the precise thickness and density of the gas, without significantly affecting the beam lifetime. The current design of a gas sheet beam profile monitor and present status are briefly reported here.

A minimally invasive gas jet profile monitor is needed to understand correlations of phase-space diffusion with dynamical resonances in a high-intensity beam, space-charge dominated beam. The Integrable Optics Test Accelerator (IOTA) at the Fermilab Accelerator Science and Technology (FAST) Facility supplies a 2.5 MeV proton beam and requires a vacuum pressure of 10^{-11} torr throughout the ring. The

pressure in the region in which the gas sheet beam profile monitor will be located can be increased to 10^{-8} torr. Thus, it is crucial to optimize the sheet divergence and gas density. Various nozzle and skimmer configurations for gas injection was simulated, as well as the proton beam and gas interaction. With a high Knudson number in ultra-high vacuum conditions, a molecular flow regime can be assumed. Gas molecules in a reservoir will traverse a nozzle and have a certain distribution entering a lower pressure region. For a cylindrical capillary tube with length l and diameter d, the number of atoms per solid angle exiting can be described by a cosine law distribution. The angular distribution pattern is only dependent on the geometry of the nozzle, i.e. the length and diameter. The existing gas density is proportional to the reservoir gas density and geometry of the orifice. For a larger length to diameter ratio the exit pattern has a 'beaming effect', as demonstrated in Clausing's diagram of angular distribution for l = 2 below.

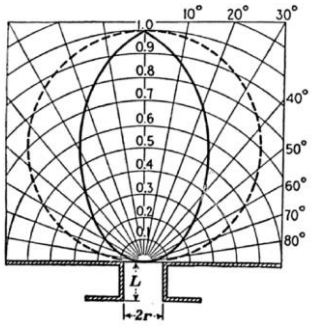

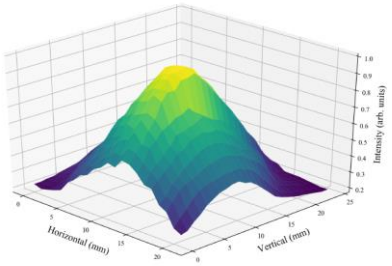

Figure 3: 2D scan of a single nozzle located 4.52 mm away.

It is assumed that a rectangular capillary can be approximated by a superposition of cylindrical tubes. Thus, the minor axis of the rectangle (i.e. the width), is like that of a cylindrical tube diameter, so that the angular distribution will be the same. Therefore, a gas sheet of a certain thickness can be formed. A skimmer can be used to select the core of the molecular beam.

The experimental gas-jet set-up is shown below.

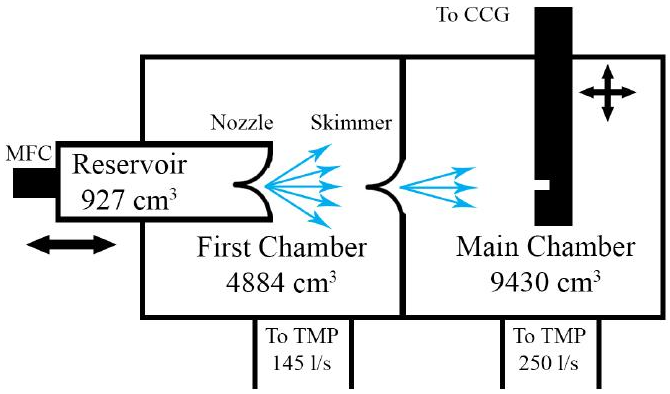

Figure 1: Sketch of apparatus setup.

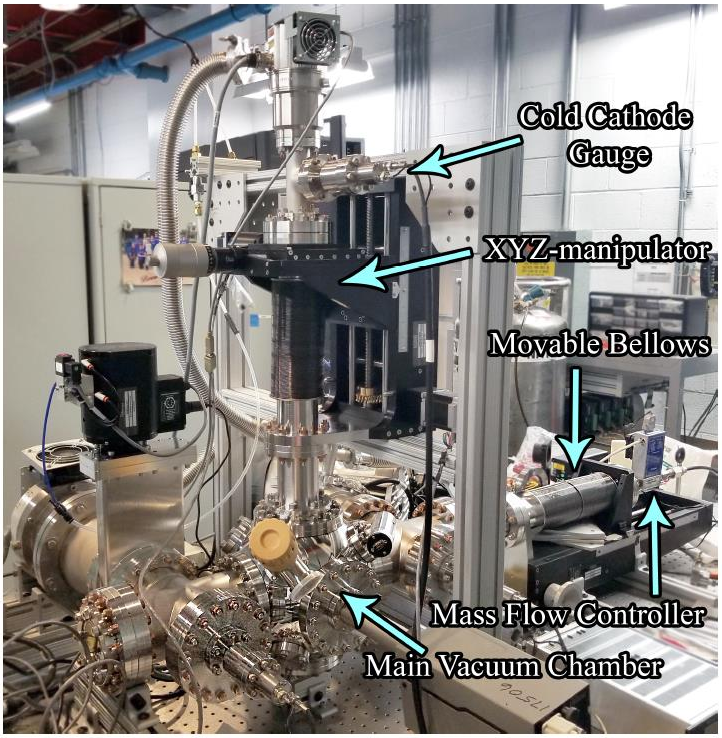

Figure 2: Gas Sheet Profile Monitor Test Stand.

A simulation of the rectangular capillary was carried out. Gas distribution with varying nozzle-skimmer distances shows that as the distance between the nozzle and skimmer decreases, the distribution in the tails of the sheet becomes more prominent. However, the density in the core increases. The gas distribution along the minor axis at various skimmer offsets, with the same detector plane

locations. shows that somewhere between an offset of 0.1mm and 0.5mm the intensity of the sheet drops by an order of magnitude. the intensity of the core decreases with increasing distance from the skimmer. At 50 mm downstream there is a noticeable increase in the FWHM for an offset of 0.5 and 1.0 mm. With no offset and the nozzle-skimmer distance at 25 mm, the FWHM of the sheet measured 100mm downstream is 0.41 mm. Using the small angle approximation, the divergence of the sheet is 0.002 radians. The half-intensity angle is expected to be 0.84 mrad. Thus, the expected FWHM at detector plane four is 0.22 mm. This is likely due to the bin size in the simulation or the assumption that a rectangular capillary is a superposition of cylindrical tubes is not entirely valid.

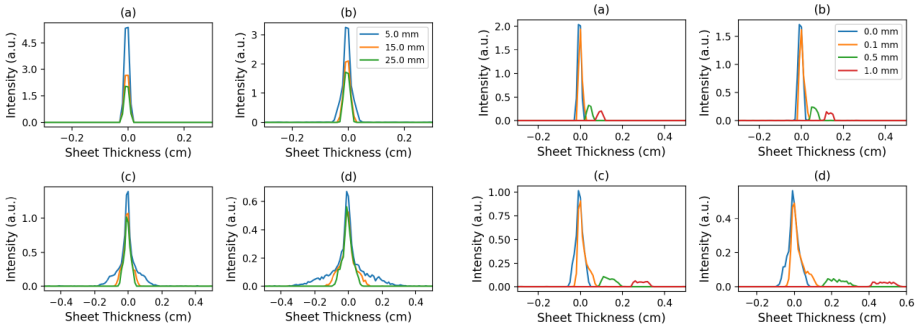

Gas distributions with various nozzle-skimmer distances and skimmer offsets are shown above.

Beam-gas interaction: A large effect due to space-charge is expected in IOTA as a result of the beam energy (2.5 MeV) and current (8 mA). Simulations of the beam-gas interaction have been performed using Warp code, which accurately models the ionization process and space-charge, to quantify the effect of space-charge as well as extraction electrode strength on the expected signal.

Simulation Parameters: A beam with a Gaussian distribution (x:y = 3:5mm) was injected. The gas sheet was approximated by 150 containers of nitrogen gas with dimensions 70x0.2x0.2 mm (x, y, z) offset from each other in y and z by 0.2mm so that a sheet extending 1:5 cm in y, rotated by 45 with respect to the z-axis was formed. Four annular electrodes, each with an inner diameter of 2.5 cm, an outer diameter of 3.0 cm, and length of 0.5 cm were placed at y positions of 2.5, 2.5, 3.5, and 4.5 cm, centered in z with the gas sheet. The electrodes were biased at +500, -500, -1000, and -1500V from bottom to top in order to direct the plasma ions toward a virtual detector. The gas density was set to 4 x 10^{11} cm-3 and the cross section for ionization is 7.19 x10^{-17} cm2. The distribution of ions was recorded at various y positions extending up to 2.5 cm over the course of the beam pulse (1.77 μs). The distribution in x of the ions should match the distribution in x of the beam, and the distribution in z of the ions should match the distribution in y of the beam,

with some smearing coming from the sheet thickness, due to the 45 degree angle between the beam and the sheet.

Simulation Results: The x and z distributions of all ions that passed through a slice in y between 2.39 and 2.50 cm (chosen based on ion velocity so that no macroparticles pass through without being counted) shows that the width of the distribution of ions does not match in either transverse direction to that of the beam. This is due to both space-charge and the strength of the extraction electrodes. The ion distribution more closely matches that of the beam closer to the beam center. Also, of note is that roughly half of all plasma ions created during a single beam passage do not make it to the virtual detector position (y = 2:5 cm) during the revolution period of the beam. This indicates a potential issue with detector pileup that will need to be addressed in the readout electronics. Further studies are underway to optimize the strength of the extraction electrodes and quantify the effect of space-charge and electrode strength on the signal distribution.

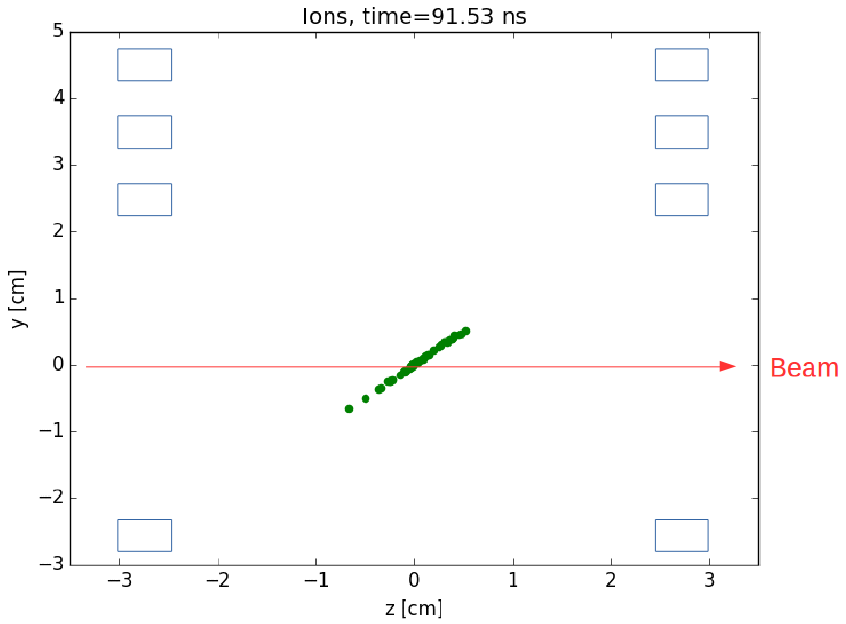

Figure above shows simulation domain in the y-z plane. The green dots are ion macroparticles generated by the beam (direction shown in red) interacting with the gas (not shown). The cross section of the electrodes are outlined in blue. This snapshot was recorded 91.53 ns into the simulation.

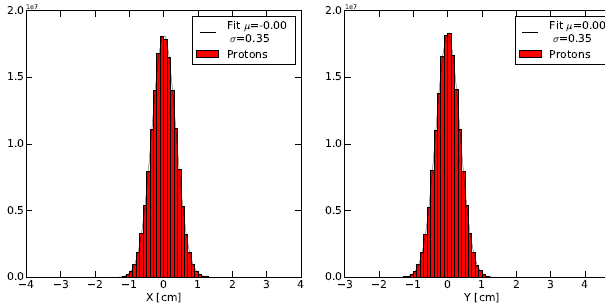

Transverse distributions are shown above for the beam (x – left, y –right), with Gaussian fits.

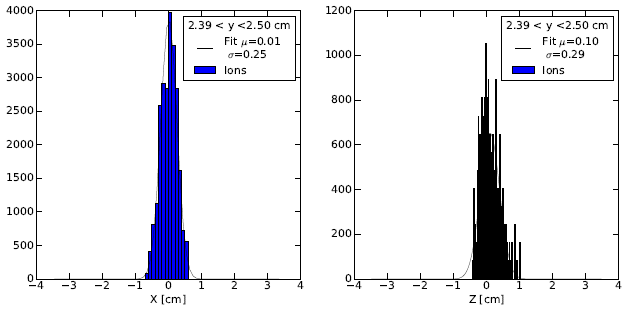

Transverse distributions (x – left, z – right) for all ions to have passed through a slice in y between 1.50 and 1.61 cm over the course of the beam pulse, with Gaussian Fits are shown above.

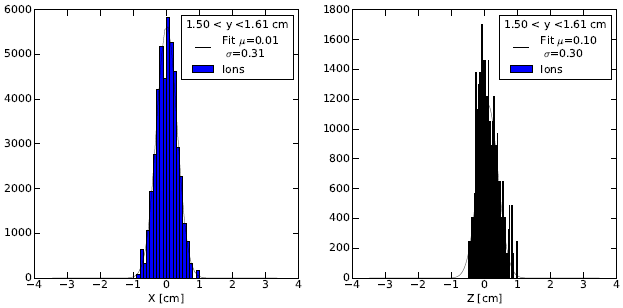

Transverse distributions (x – left, z – right) for all ions to have passed through a slice in y between 2.39 and 2.50 cm over the course of the beam pulse, with Gaussian fits are shown above.

In summary, simulations of the beam-gas interaction have been done. MolFlow+ simulations were used to estimate a gas sheet distribution for various configurations of nozzles and skimmers. Construction of a test bench is underway at

FAST at Fermilab. This will be used to validate the simulation results for various nozzle and skimmer configurations. Eventually, the monitor will be tested elsewhere at Fermilab's accelerator complex e.g. at the Main Injector or PIP-II injector stand, until a proper proton/ion source is built for IOTA.

3. PRODUCTS

Conference papers, reports and presentations:

- ***a.*** *Development of a gas sheet beam profile monitor for IOTA,* S. Szustkowskiy1, S. Chattopadhyay, D. Crawford, B. Freemire, 9th International Particle Accelerator Conference IPAC2018, Vancouver, BC, Canada JACoW Publishing, ISBN: 978-3-95450-184-7 doi:10.18429/JACoW-IPAC2018-WEPAL065
- ***b.*** *Gas jet profile monitor for use in iota proton beam,* S. Szustkowski, S. Chattopadhyay, D. Crawford, B. Freemire, 6th International Beam Instrumentation Conference IBIC2017, Grand Rapids, MI, USA JACoW Publishing ISBN: 978-3-95450-192-2 doi:10.18429/JACoW-IBIC2017-WEPCC05
- ***c.*** *Skimmer-nozzle configuration measurements for a gas sheet beam profile monitor*, S. Szustkowski, S. Chattopadhyay, D. Crawford, B. T. Freemire, NPAC 2017, Chicago, Illinois.
- ***d.*** *Nonlinear tune-shift measurements in the integrable optics test accelerator,* S. Szustkowski, A. Valishev, N. Kuklev, A. Romanov, S. Chattopadhyay, submitted to NPAC 2019, Michigan State University, East Lansing, Michigan, August 2019.

4. PARTICIPANTS

1. **Name:** Swapan Chattopadhyay
2. **Project Role:** Principal Investigator
3. **Nearest person months worked:** 3
4. **Contribution to Project:** technical leadership of the task on simulation, design and fabrication of gas jet diffusion monitor and IOTA nonlinear tune-shift measurements

1. **Name:** Sebastian Szustkowski
2. **Project Role:** Graduate Research Assistant
3. **Nearest person months worked:** 24
4. **Contribution to Project:** studied IOTA beam optics and nonlinear lattice and helped design and developed gas jet monitoring system

1. **Name:** Ben Freemire
2. **Project Role:** postdoc
3. **Nearest person month worked:** 18
4. **Contribution to Project:** Design and fabrication of gas jet monitoring system